# AMPLITUDE ANALYSIS AND MODELING OF PEACEFUL NUCLEAR EXPLOSION RECORDINGS

Igor B. Morozov, Scott B. Smithson, Hongyan Li, and Joel N. Duenow

University of Wyoming

Sponsored by Defense Threat Reduction Agency

Contract No. DTRA01-01-C-0057

## ABSTRACT

For a number of years, in cooperation with the Centre of Regional Geophysical and Geological Research (Centre GEON), Moscow, Russia, the Reflection Seismology group at the University of Wyoming has been analyzing the unique recordings of Peaceful Nuclear Explosions (PNEs) in Russian Eurasia. Recent studies included imaging two-dimensional velocity, reflectivity, and P-wave attenuation of the upper mantle to ~700-km depth, interpretation of high-frequency scattering, and seismic coda. In this new project, we focus specifically on the analysis of the spectral properties of *Lg*, crustal and upper mantle attenuation using the spectral and coda decay information extracted from the PNE records.

At this early development stage of the project, we present plans of data measurement and modeling techniques. Relative spectral amplitudes for both attenuation and coda studies are derived using multi-taper techniques designed to increase the stability of the estimates in respect to the effects of noise. Owing to a generalized formulation of the spectral estimation problem (implemented in an object-oriented code using C++ programming language), virtually the same technique is used for the measurements of both *P*-wave spectral attenuation (t*), *Lg Q*, and *Lg* coda *Q*. Preliminary results using five of the available PNE profiles show *Lg* coda *Q* values similar to those obtained previously in our studies of a part of profile QUARTZ. From these measurements, we plan to produce crustal and upper mantle *Q* values that are required for large-scale simulation of propagation of the regional phases (*Lg*, *Pg*, *P*, and *S*) across Northern Eurasia

Our current modeling effort is targeting simulation of a realistic, three-component coda created by a distant PNE source. Since, as we have argued previously, three-dimensional (3-D) simulations are required for a correct description of short-period coda of PNE arrivals, we perform our modeling in 3-D by employing a single-scattering (Born) approximation. To achieve this, we first pre-compute the Green's functions for the source and for the scattering point using 1- or 2-D finite-difference simulation, and then convolve them multiplied by the surface scattering potential in order to obtain the desired scattered response. This modeling technique both correctly accounts for 3-D geometric spreading, for the complexity and three-component character of the wavefield, and also captures coda amplitude irregularities caused by heterogeneity of the scattering potential (associated, for example, with variations in topography, crustal faults, or boundaries of sedimentary basins). We expect that such modeling could be used to calibrate our measurements.

## OBJECTIVES

In cooperation with Centre GEON, Moscow, Russia, the University of Wyoming has obtained a substantial part of the unique Deep Seismic Sounding (DSS) data including systematic and continuous profiling of Peaceful Nuclear Explosions (PNEs) in Northern Eurasia (**Figure 1**). Along with reversed recording of the PNEs to over 3000-km ranges, 30 to 80 chemical explosions were recorded in each of the ultra-long profiles, making these datasets unparalleled in terms of both detailed coverage of the crust and upper mantle and also as comprehensive collections of seismic recordings of explosions at regional distances. Recent studies of the data included imaging two-dimensional velocity, reflectivity, and P-wave attenuation of the upper mantle to ~700-km depth, interpretation of high-frequency scattering and seismic coda. In this new project, we focus specifically on the analysis of the spectral properties of *Lg*, crustal and upper mantle attenuation using the spectral and coda decay information extracted from the PNE records.

At this early stage of the project, we present plans of data measurement and modeling techniques. The principal objectives of this work include:

1) Development of amplitude and spectral measurement techniques taking into account the character of PNE recordings using portable, 3-component, densely spaced instruments. These methods include measurements of spectra, spectral ratios, relative amplitudes, and amplitude decay parameters for the different phases. Below, we describe our techniques for estimations of power spectra and effective attenuation.
2) Development of methods for modeling of the PNE waveforms and amplitudes, with accounting for the complexity of the observed waveforms and propagation paths. Specifically, we need to develop modeling methods for short-period (~1-2 Hz) crustal-guided phases (*Pg*, *Lg*) propagating to ~2000 km along crustal paths that are heterogeneous in a 3D sense. Since the straightforward 3D modeling problem of this scale is not tractable and also not supported by sufficient data at present, we propose several approximate approaches that could produce interpretable and useful results. Below, we describe our ongoing work on one of these approximations of the PNE arrival coda using the first-order Born scattering in 3D.

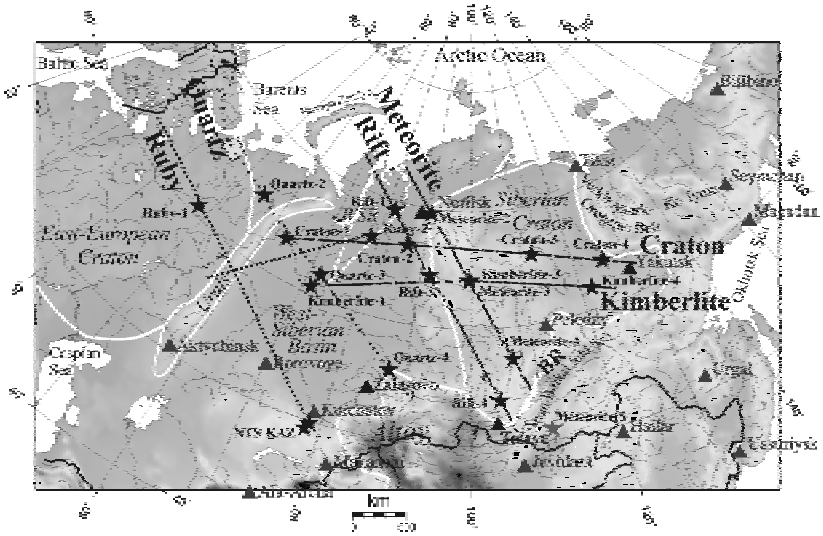


**Figure 1. DSS PNE profiles under study at the University of Wyoming: QUARTZ, CRATON, KIMBERLITE, RIFT, METERORITE, and RUBY (two lines, obtained recently). Large stars are the PNEs; small stars (for profile QUARTZ only) are the chemical explosions. Profile RUBY is shown schematically. The coordinates and other parameters of the PNEs used in these profiles were reported by Sultanov et al (1999). White contours show the major tectonic units (labeled: WSR – West Siberian Rift, BR – Baikal Rift). Note the extent of systematic, continuous profiling, with PNEs detonated at the intersections of the 3000–4000-km long profiles. The profiles are close to some of the IMS stations (labeled triangles). The profile QUARTZ has been studied extensively for the upper mantle and crustal structure, for seismic coda effects and crustal reverberations. The box NW of PNE QUARTZ 2 indicates the area where crustal attenuation was measured using coda amplitude analysis.**

## RESEARCH ACCOMPLISHED

Below, we describe our approaches to the attribute extraction and approximate 3D coda modeling. As this is work in progress, we concentrate on the methodologies and applications in the project.

**Measurements of spectra and effective *Q* from PNE records.**

Relative spectral amplitudes for both attenuation and coda studies are derived using a broad class of multitaper techniques similar to the one used by Xie et al. (1988). Multiple spectral estimates in shorter sub-windows increase the stability of the estimates in respect to the effects of noise (Figure 2). This increase is achieved at the expense of reduced spectral resolution resulting from using shorter time sub-windows for spectral analysis. Such a reduction, however, is quite acceptable for PNE records in which the signal typically exhibits little coherency over time period exceeding ~5 s; consequently, we estimate that a time window of ~5 s is the appropriate choice for spectral sampling. This choice results in a ~0.2 s resolution of the spectra and allows us using 4-8 sub-windows for *Lg*, *Sn*, and *Pg*. Also, most importantly, this generalized multiple tapering technique provides for an estimation of the effective spectral decay (attenuation) within the analysis time gate (Figure 2).

Our spectral estimation method is an extension of the common spectrum technique described by Morozov et al. (1998). First, in each of the tapered sub-windows *i*, we compute the amplitude FFT spectrum of the signal, $A_i(f)$ (Figure 2). By selecting a set of pairs of sub-windows, $(i,j)$ (choosing this set is yet another option of the algorithm), we form their associated spectral ratios: $SR_{i,j}=A_i(f)/A_j(f)$. By assuming the usual model of the spectra:

$$A_i(f) = A_0(f)e^{-\pi f t_i / Q},$$

and taking a logarithm of the spectral ratios, we obtain a linear inverse problem for $1/Q$:

$$\ln SR_{i,j}(f) = -\frac{\pi f}{Q}(t_i - t_j). \qquad (1)$$

This linear system (for a range of frequencies *f* and pairs of time sub-windows *i* and *j*) is solved using the Least Squares approach. This method is also suitable to invert for a frequency-dependent attenuation: by replacing $1/Q$ in

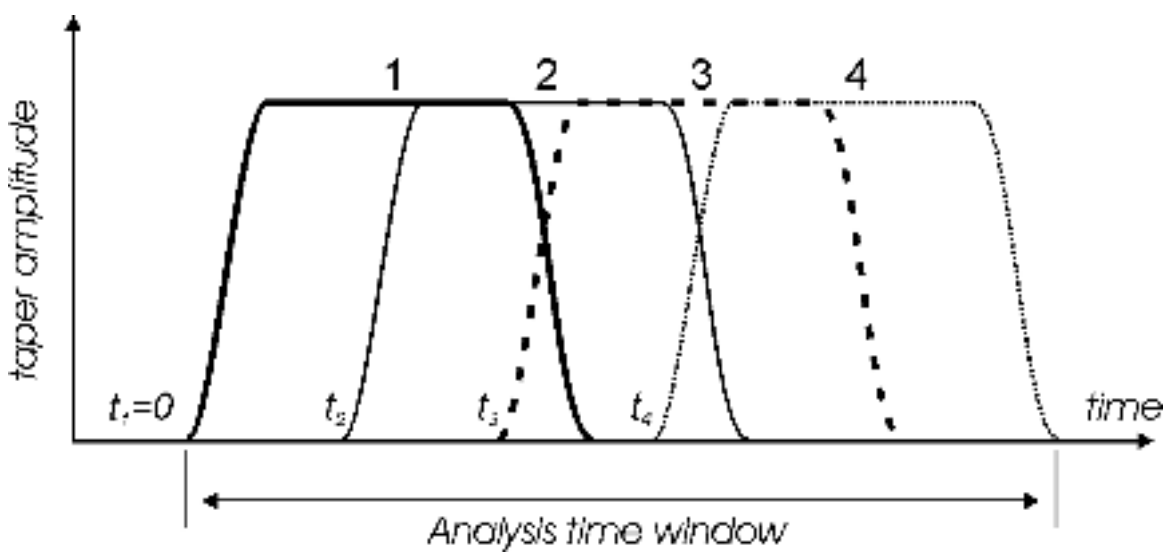


**Figure 2.Multiple-taper spectral analysis windows. The spectral analysis time gate is subdivided into a number of overlapping sub-windows (libeled with numbers). Although the tapers do not have to be trapezoidal and equally spaced, in this example, we are using four identical Hanning windows. Increasing number of tapers improves the statistical significance of the results at the expense of spectral resolution (reduced because of using shorter FFT analysis gates).**

equation (1) with $1/Q_0 + \gamma f$, we obtain:

$$\ln SR_{i,j}(f) = -\frac{\pi f}{Q_0}(t_i - t_j) - \gamma f^2 (t_i - t_j), \tag{2}$$

which is also a linear inverse problem in respect to $1/Q_0$ and $\gamma$. In order to avoid complications caused by spectral holes, we exclude from the above analysis the frequencies at which any of the (normalized) spectra $A_i(f)$ becomes lower than some predefined threshold (Morozov et al., 1998).

After the (possibly, frequency-dependent) value of $1/Q$ is estimated, the final "common", time-independent, spectrum $A_0(f)$ is estimated simply by averaging the sub-window spectra corrected for the attenuation:

$$A_0(f) = \frac{1}{N}\sum_{i=1}^{N} A_i(f) e^{\pi f t_i / Q} . \tag{3}$$

Here, N is the number of time sub-windows (Figure 2). Note that spectral holes do not need to be excluded from expression (3), and thus we obtain a uniform estimate of both the spectral amplitude and $Q$ throughout the entire frequency range.

A three-component analog of the expressions (1-3) above can be obtained by using spectra averaged over the three displacement directions:

$$A_0(f) = \overline{A}_0(f) = \sqrt{\sum_{i=x,y,z} (A^i)^2} .$$

Our preliminary tests of this procedure using synthetic data and records from profile Kimberlite show that the resulting estimates of $Q$ are stable and the *Lg* $Q$ (spectral attenuation across the *Lg* window) and *Lg* coda $Q$ are similar to each other. Preliminary results using five of the available PNE profiles show *Lg* coda $Q$ values similar to those obtained previously in our studies of a part of profile QUARTZ. From these measurements, we plan to produce crustal and upper mantle $Q$ values that are required for large-scale simulation of propagation of the regional phases (*Lg*, *Pg*, *P*, and *S*) across Northern Eurasia

**Simulations of PNE arrival coda in 3D.**

The motivation for our coda modeling effort is illustrated in Figure 3. As a number of previous attempts for finite-difference modeling of the coda of long-range PNE arrivals (Tittgemeyer, 1996; Ryberg et al., 2000,) indicated, neither 1D nor 2D simulations are able to explain the observed amplitude patterns of PNE arrivals at regional to teleseismic distances (Morozov and Smithson, 2000; Morozov, 2001). Therefore, three-dimensional (3D) simulations are required for a correct description of short-period coda of PNE arrivals (Figure 3).

Our current modeling is targeting simulations of a realistic, three-component wavefield recorded from a distant PNE source. Since the full 3D modeling problem is not tractable at present, we perform our modeling by employing a single-scattering (Born) approximation. This modeling technique both correctly accounts for 3D geometric spreading, for the complexity and three-component character of the wavefield. Also, by using such an approximation, we could potentially identify regions of increased scattering in the PNE records and associate them with the major tectonic or topographic features (such as crustal faults, mountain ranges, or boundaries of sedimentary basins; Figure 4). Thus we expect that such modeling could be used to calibrate the above measurements.

Scattering, as shown in Figure 4, is dominated by the out-of-plane effects, and it cannot be modeled correctly by conventional 2D numerical modeling. Nevertheless, as we are mainly interested in RMS average energy decay in the coda, we can estimate the recorded signal at any surface point by convolving the incident wavefield with an "empirical Green's function" that would describe the propagation of scattered waves, multiplied by some "scattering potential" (Revenaugh, 1995):

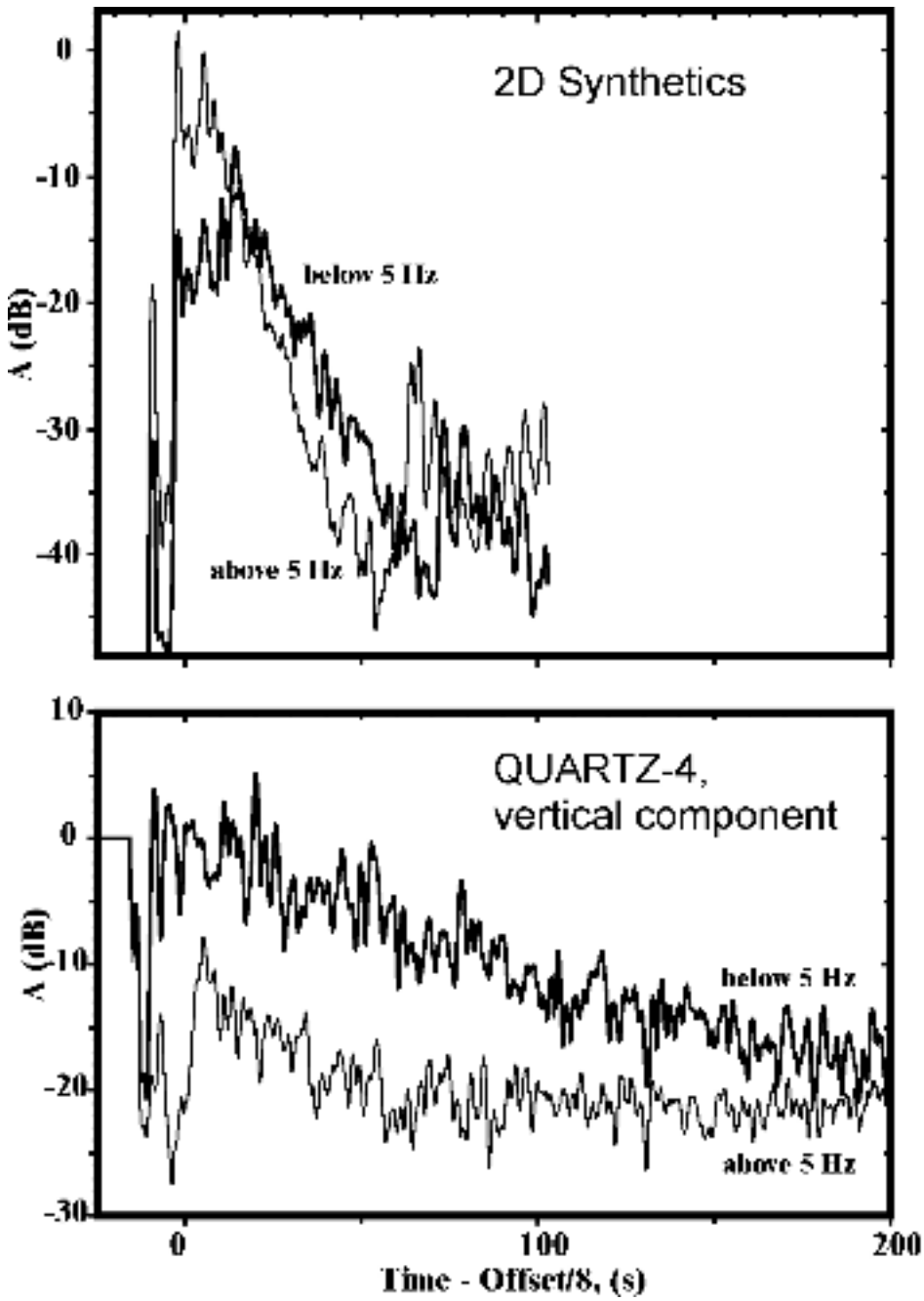


**Figure 3. Comparison of the amplitude decay observed in PNE QUARTZ-4 (bottom) and modeled using an elastic 2D finite-difference method (modelling performed by Lars Nielsen, University of Copenhagen; unpublished). Note that the observed coda is significantly longer than the one obtained from 2D synthetics, both at higher and lower frequencies. As we argue (Morozov and Smithson, 2000), only some kind of 3D simulation could provide an adequate model of the coda.**

$$\tilde{u}(r,t) = R \square dsdt \square A(s) u(s,t \square) * G(s,t \square r,t), \qquad (1)$$

where *s* is the surface integration point, u() is the source function, and *A* is the scattering potential, and R is the receiver factor, and '*' denotes time convolution (Figure 4).

Both the direct wave response at point *S* and the Green's function *G*(…) in equation (1) can be estimated from 2D or 1D synthetics. At present, we precompute the Green's functions for the source and for the scattering point using the 1D finite-difference modeling program modified after Fuchs and Muller (1971). The scattering potential in equation (1) can be simulated either as a stochastic function or based on an empirical correlation with topography, crustal faulting, and seismicity (Revenaugh, 1995, 2000).

For any recording point at the surface, *R*, we simulate the seismic trace coda by attributing its form to the effect of point scattering of seismic waves from surface scattering points (Figure 4). A seismic wave travels outward from the seismic source S. Part of this energy is received at scatter point *Sc* and reflected from the point to receiver R. The waveform recorded at R is a function of the source waveform, source-scatterer distance, and scatterer-receiver distance. In this simulation, the source waveform is a synthetic IASP-91 seismic section. Several scatterers may be arranged to simulate various geologic scattering bodies; for instance, a linear array of scatterers may simulate a mountain range (Figure 4), a boundary of a sedimentary basin, or a coastline. We specify a linear array of receivers to act as a seismic line.

The synthetic coda due to surface point-scattering effects is computed by summing over the convolution of two synthetic traces for each scatterer-receiver pair. The first trace represents the seismic signal at the offset of the scattering point from the seismic source. The second trace contains the signal at the offset of the receiver from the scattering point (Figure 4). The traces are determined from the synthetic seismic section using a □-*p* interpolation

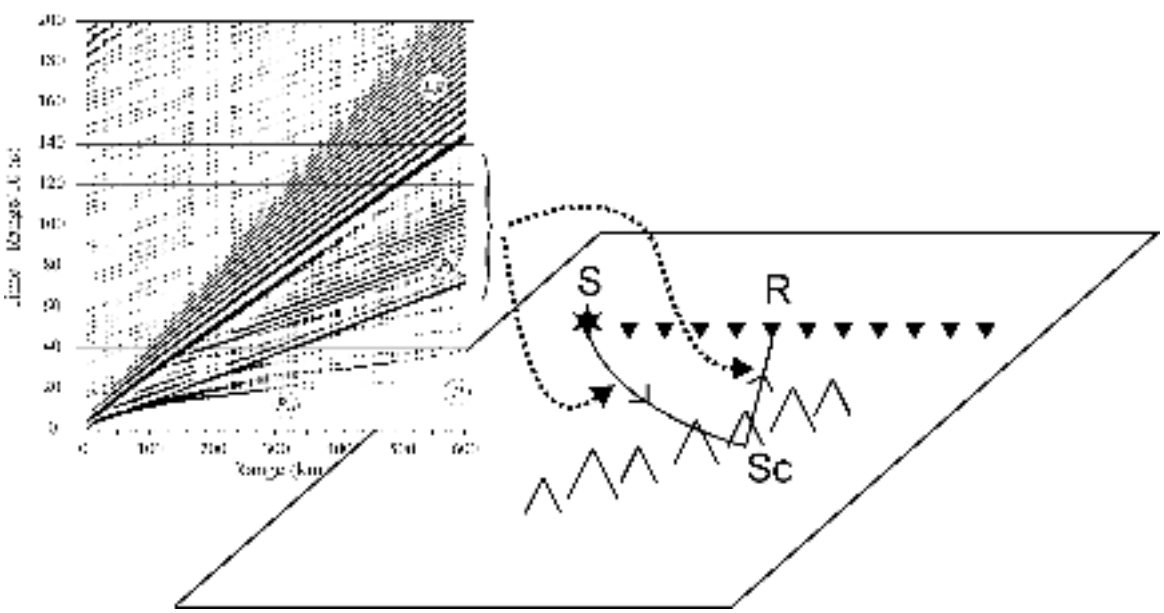


**Figure 4. Simulation of first-order scattering responses. The wavefield at receiver location ® is approximated as a combination of the direct wavefield from the source (S) and an integral over the positions of the scatterers (*Sc*) located near the Earth's surface. At present, we approximate the direct source field and both legs of the scattering path *S_Sc_R* using an empirical Green's function (shown here as a data section) computed using a 1D reflectivity synthetic (Fuchs and Muller, 1971). Note that since a dominant contribution to the coda comes from the waves trapped within the crustal layers and propagating generally horizontally, their amplitude decay with distance is compensated by the increasing area of scattering (Morozov and Smithson, 2000). As a result, coda energy is collected from a large area and its decay is slow.**

routine which allows us to compute the trace values more accurately because a more accurate offset value is used in each calculation. Rather than using the nearest trace to the offset distance from the synthetic section for each of the two traces in the convolution, new traces are interpolated between traces of the synthetic section for the source-scatterer and scatterer-receiver distances and convolved. The source-scatterer and scatterer-receiver traces, when convolved, give the scattering response at receiver *R*. These convolution calculations are repeated for each scatterer-receiver pair. All the resulting convolved trace values from each scatterer-receiver pair are summed together at each receiver to give the total response due to point scattering.

**Implementation**

The above procedures are implemented in a very general form of programmable seismic processing flows (Morozov and Smithson, 1997; http://w3.uwyo.edu/~seismic/sia) allowing the use of arbitrary configurations of receivers and a variety of choices of scattering regions. In principle, the procedure also allows iterating the scattering steps thereby extending our modeling beyond the single-scattering Born approximation. However, such iteration would require a significantly greater computing power and thus it still has not been investigated.

In developing our signal processing and modeling approaches, a considerable effort is applied to achieving sufficient portability and scalability of the methods. Owing to a highly generalized formulation of the spectral estimation problem (implemented in an object-oriented code using C++ programming language), virtually the same technique is used for the measurements of both *P*-wave spectral attenuation ($t^*$), *Lg Q*, and *Lg* coda *Q*. The codes are completely portable and implemented on several platforms ranging from a multi-processor SGI and Sun systems to a PC Linux notebook (interestingly, the latter yielding the highest performance!). The codes include hundreds of useful C++ classes, over 140 seismic processing tools, and are equipped with a system maintenance package and automated on-line documentation (http://w3.uwyo.edu/~seismic/sia). In the near future, we are planning to extend the package with a capability for operation on multiprocessor platforms (Beowulf clusters) using the Message Passing Interface (MPI).

## CONCLUSIONS AND RECOMMENDATIONS

In this report, we present our ongoing development of methods for quantitative amplitude and spectral analysis and modeling of PNE arrivals recorded by the Deep Seismic Sounding profiles in the former Soviet Union. The importance of this research is emphasized by the great variety of the tectonic structures covered by the profiling and also by the fact that DSS recordings cover largely aseismic regions of Northern Eurasia where virtually no other data is available for seismic calibration ( ). The DSS data sets contain abundant 3-component recordings of the full spectrum of regional phases that hold significant potential for seismic calibration and discrimination. At present, we have implemented and tested on synthetics procedures for (1) spectral measurements of PNE arrivals using multiple tapering and allowing estimations of (optionally) frequency-dependent effective attenuation, and (2) approximate modeling of the amplitude decay of PNE arrivals in 3D using the first-order, Born approximation.

Further research will involve: (1) space and time-variant measurements of the amplitude decay, (2) interpretation of the resulting database and inversion of the amplitude and spectral decay parameter for variations in the regional crustal attenuation structure and correlation with tectonics; (3) modeling of *Lg* propagation using an extended, 3D variant of the Generalized Screen Propagator (e.g., Wu et al., 2000), and (4) integration of the resulting *Lg* waveforms with our surface scattering model. The above studies should result in a comprehensive modeling capability that could be utilized for interpretation of both average and region-specific character of regional wave propagation in Northern Eurasia.

## REFERENCES

Morozov, I. B. (2001). Comment on “High-frequency wave propagation in the uppermost mantle” by T. Ryberg and F. Wenzel, J. Geophys. Res., 106, 30,715-30,718.

Morozov, I., B., E. A. Morozova, S. B. Smithson, and L. N. Solodilov, 1998. 2D image of seismic attenuation beneath the Deep Seismic Sounding profile QUARTZ, Russia, Pure Appl. Geoph, 153, 311-343.

Revenaugh, J. (1995). The contribution of topographic scattering to teleseismic coda in Southern California, Geophys. Res. Lett., 22, 543-546.

Ryberg, T., M. Tittgemeyer, and F. Wenzel (2000). Finite-difference modelling of P-wave scattering in the upper mantle, Geophys. J. Int, 141, 787-800.

Sultanov, D. D., J. R. Murphy, and K. D. Rubinstein (1999). A seismic source summary for Soviet Peaceful Nuclear Explosions, Bull. Seism. Soc. Am., 89, 640-647.

Tittgemeyer, M., F. Wenzel, K. Fuchs, and T. Ryberg (1996). Wave propagation in a multiple-scattering upper mantle—observations and modeling, Geophys. J. Int., 127, 492-502.

Wu, R.-S., S. Jin, and X.-B. Xie (2000). Energy partition and attenuation of *Lg* waves by numerical simulation using screen propagators, Phys. Earth. Planet. Inter., 120, 227-243.

Xie, J., et al., (1998), Interpretation of high-frequency coda at large distances: Stochastic modeling and method of inversion. Geophysical Journal.95, 579-595.